Pflugers Arch - Eur J Physiol (2012) 464:33–41
DOI 10.1007/s00424-012-1074-2

INVITED REVIEW

Mitochondria and chromaffin cell function

Javier García-Sancho · Antonio M. G. de Diego · Antonio G. García

Received: 14 December 2011 / Revised: 5 January 2012 / Accepted: 9 January 2012 / Published online: 27 January 2012

Abstract Chromaffin cells are an excellent model for stimulus–secretion coupling. Ca^{2+} entry through plasma membrane voltage-operated Ca^{2+} channels (VOCC) is the trigger for secretion, but the intracellular organelles contribute subtle nuances to the Ca^{2+} signal. The endoplasmic reticulum amplifies the cytosolic Ca^{2+} ($[Ca^{2+}]_C$) signal by Ca^{2+}-induced Ca^{2+} release (CICR) and helps generation of microdomains with high $[Ca^{2+}]_C$ (HCMD) at the subplasmalemmal region. These HCMD induce exocytosis of the docked secretory vesicles. Mitochondria close to VOCC take up large amounts of Ca^{2+} from HCMD and stop progression of the Ca^{2+} wave towards the cell core. On the other hand, the increase of $[Ca^{2+}]$ at the mitochondrial matrix stimulates respiration and tunes energy production to the increased needs of the exocytic activity. At the end of stimulation, $[Ca^{2+}]_C$ decreases rapidly and mitochondria release the Ca^{2+} accumulated in the matrix through the Na^+/Ca^{2+} exchanger. VOCC, CICR sites and nearby mitochondria form functional triads that co-localize at the subplasmalemmal area, where secretory vesicles wait ready for exocytosis. These triads optimize stimulus–secretion coupling while avoiding propagation of the Ca^{2+} signal to the cell core. Perturbation of their functioning in neurons may contribute to the genesis of excitotoxicity, ageing mental retardation and/or neurodegenerative disorders.

Keywords Mitochondria · Chromaffin cell · Calcium · Mitochondrial calcium uniporter · Aequorin · Calcium microdomains · Exocytosis

Abbreviations

ER	Endoplasmic reticulum
$[Ca^{2+}]_C$	Cytosolic Ca^{2+} concentration
$[Ca^{2+}]_M$	Mitochondrial Ca^{2+} concentration
$[^TCa]$	Total calcium concentration
CICR	Calcium-induced calcium release
HCMD	High Ca^{2+} microdomains
VOCC	Voltage-operated Ca^{2+} channels
MCU	Mitochondrial Ca^{2+} uniporter
SERCA	Sarcoendoplasmic reticulum Ca^{2+}-activated ATPase
SOC	Store-operated Ca^{2+} entry also known as capacitative Ca^{2+} entry

Introduction

The adrenal gland is responsible for the adjustment of many physiological functions to demanding or stressful conditions through secretion of the catecholamines adrenaline and noradrenaline. In addition, Ca^{2+} triggering of adrenaline secretion from chromaffin cells has been used as a general model for *stimulus–secretion* coupling [20]. According to the initial formulation, stimulus promotes Ca^{2+} entry, which increases the cytosolic Ca^{2+} concentration ($[Ca^{2+}]_C$) and

This article is published as part of the special issue on "Cell-specific roles of mitochondrial Ca^{2+} handling."

J. García-Sancho (✉)
Instituto de Biología y Genética Molecular (IBGM),
Universidad de Valladolid and CSIC,
c/Sanz y Forés, 3,
47003, Valladolid, Spain
e-mail: jgsancho@ibgm.uva.es

A. M. G. de Diego · A. G. García
Instituto Teófilo Hernando; Departamento de Farmacología y Terapéutica; Servicio de Farmacología Clínica,
Instituto de Investigaciones Sanitarias del Hospital de la Princesa;
Facultad de Medicina, Universidad Autónoma de Madrid,
Madrid, Spain

triggers exocytosis [20, 21]. Later studies showed that the genesis of the $[Ca^{2+}]_C$ signal includes subtle nuances contributed by the intracellular Ca^{2+}-handling organelles [5, 8, 24, 25]. To begin with, Ca^{2+} entering through the plasma membrane Ca^{2+} channels is buffered by cytosolic Ca^{2+} buffers, so that the increase of $[Ca^{2+}]_C$ is much less than expected. On the other hand, organelles interrupt physically the diffusion pathways and make them much longer and tortuous. In addition, many organelles avidly take up Ca^{2+} and drain the Ca^{2+} wave; on the contrary, other organelles amplify the $[Ca^{2+}]_C$ signal by releasing Ca^{2+} [3, 5, 7, 55]. In this way high $[Ca^{2+}]_C$ microdomains (HCMD) are built at the secretion site whereas $[Ca^{2+}]_C$ near the resting level is preserved at the cell core. Mitochondria play a prominent role in shaping the $[Ca^{2+}]_C$ signal in chromaffin cells [24]. On the other hand, changes of Ca^{2+} concentration in the mitochondrial matrix ($[Ca^{2+}]_M$) modify the rate of respiration [27, 32, 47, 49, 51] and, when excessive, can trigger cell death [22].

Calcium buffering differs among different subcellular compartments

It is a general observation that calcium binds avidly to endogenous Ca^{2+}-binding proteins in all the intracellular compartments including the cytosol, so that the total calcium concentration ($[^TCa]$) is always much larger than the ionised one ($[Ca^{2+}]$). The ratio $d[^TCa]/d[Ca^{2+}]$ or *calcium-binding capacity* [40] quantifies this buffering effect. Differences in buffering power among different compartments do not generate $[Ca^{2+}]$ gradients but differences in their $[^TCa]$. On t4he other hand, the calcium content of a given organelle determines his potential weight on the generation of global $[Ca^{2+}]_C$ signals. For example, the magnitude of the $[Ca^{2+}]_C$ peak generated by Ca^{2+} release from a given organelle depends on the ratio of the calcium-buffering powers ($B_{organelle}/B_{cytosol}$) and the volume ratio ($V_{organelle}/V_{cytosol}$). Other parameters that should be considered when evaluating the influence of organellar Ca^{2+} transport on Ca^{2+} signalling are kinetics (faster flows generate neater $[Ca^{2+}]_C$ signals) and distance to the Ca^{2+} target (closer location gives stronger effect).

The *calcium-binding capacity* (κ_S) of the cytosol may differ widely among different cell types. κ_S values 1,000 have been reported for myocytes [58] and various neuronal types [1, 23, 46, 54]. On the other hand, values of 40–100 have been reported for rat chromaffin cells [11, 29] and bovine chromaffin cells [40, 60, 63].

The approximate values of several relevant parameters in order to estimate the effects of calcium redistribution among different compartments are summarized in Table 1. The last column compares the size of the different Ca^{2+} pools at rest when all are expressed in the same units (in millimoles per litre of cells). It seems clear from these values that release of even a small fraction of the endoplasmic reticulum (ER) or secretory granules (SG) Ca^{2+} pools would produce a big $[Ca^{2+}]_C$ increase. This is accepted for ER, but opinions on the relevance of the secretory granules pool for cytosolic signalling are controversial. While the classical view stated that Ca^{2+} exchanges between the secretory granules pool and the cytosol are too slow to participate in $[Ca^{2+}]_C$ signalling, it has been proposed recently that secretory granules possess Ca^{2+} channels that can be activated by second messengers and that they could be activated under physiological conditions [44, 61]. The calcium contained in other acidic granules, such as lysosomes or endosomes (not shown in Table 1), could also play a role [43], although the size of this pool is much smaller. Finally, it has been proposed that the nucleus could also contain a releasable Ca^{2+} pool stored within the nuclear envelope and their invaginations to the nucleoplasm, the *nucleoplasmic reticulum*, as well as complexed inside nuclear *nanovesicles* that are below electron microscope resolution [4, 62]. The mitochondria store little or no calcium in the resting condition (Table 1), but they can take up very quickly a large amount of Ca^{2+} when $[Ca^{2+}]_C$ increases, and then release it slowly to the cytosol when $[Ca^{2+}]_C$ declines (see below).

Cytosolic Ca^{2+} buffering and diffusion in bovine chromaffin cells has been extensively studied by Neher and coworkers [40, 60, 63]. The cytosol has a total binding capacity of 4 mM, and the endogenous Ca^{2+} buffer is fast (association rate=10^{-8} $M^{-1}s^{-1}$), poorly mobile, and with low affinity for Ca^{2+} (dissociation constant=100 μM). The *calcium-binding capacity* ($d[^TCa]/d[Ca^{2+}]_C$) of the endogenous buffer is about 40. Cytosolic buffering slows down Ca^{2+} mobility to reach an apparent diffusion rate of about 10^{-7} cm^2 s^{-1}. The two-dimensional apparent diffusion coefficient is about 40 $\mu m^2 \cdot s^{-1}$ and shows inhomogeneities at

Table 1 Calcium pools in chromaffin cells

Compartment	Relative volume	$[^TCa]$ in M	Ca-binding capacity (κ_S)	$[Ca^{2+}]$ in M	Mol · l of cells^{-1} (relative size)[a]
Cytosol	0.70	$4 \cdot 10^{-6}$	40	$1 \cdot 10^{-7}$	$2.8 \cdot 10^{-6}$ (1)
Mitochondria	0.05	$1 \cdot 10^{-4}$	1,000	$1 \cdot 10^{-7}$	$5.0 \cdot 10^{-6}$ (×2)
ER	0.10	$2 \cdot 10^{-2}$	20	$1 \cdot 10^{-3}$	$2.0 \cdot 10^{-3}$ (×714)
Secretory granules	0.15	$4 \cdot 10^{-2}$	800	$5 \cdot 10^{-5}$	$6.0 \cdot 10^{-3}$ (×2,142)

Approximate figures based on published data [6, 7, 26–28, 45, 53, 59–63]

[a]In the resting condition. The figure in parentheses is expressed as fold relative to cytosol

the nuclear envelope and at the plasma membrane [37]. Brief opening of voltage-operated Ca^{2+} channels (VOCC) generates microdomains of high $[Ca^{2+}]_C$ near the mouth of the channel which can be detected in Ca^{2+} imaging measurements [40]. In such microdomains Ca^{2+} can reach concentrations as high as 10 μM and perhaps 100 μM [10, 38]. Because of rapid diffusion of Ca^{2+} towards the surrounding cytosol, $[Ca^{2+}]_C$ microdomains are very much restricted in time and space [38, 39]. The presence of mobile buffers accelerates diffusion and opposes development of HCMD [52]. For example, 50 μM fura-2 in the cytosol increases the rate of diffusion fourfold [63].

High Ca^{2+} microdomains

Ca^{2+} signalling becomes all or none at the molecular level, as very high Ca^{2+} concentrations are required to trigger Ca^{2+}-dependent processes. The $[Ca^{2+}]_C$ concentration peaks measured with Ca^{2+} probes are usually underestimated, as they represent the global value, which is the average HCMD and other cell locations with much lower $[Ca^{2+}]_C$. The probability of generation of an HCMD increases very much with the coincidence in time and space of the opening of many calcium channels. This depends on four dimensions, the three spatial coordinates (x, y and z) and time (t), which can be regarded as the degrees of freedom that oppose HCMD generation. In excitable cells, the generation of HCMD is very much favoured. The z coordinate for the calcium channels is severely restricted, as the channel has to lie within the plasma membrane plane. In addition, channels may tend to pack together in clusters, thus introducing additional restrictions on x and y. Finally, because the channel openings are synchronized by the action potential, the t dimension is also severely restricted. The result is that the probability for HCMD generation at the subplasmalemmal region and coincident in time with action potentials is very much increased in excitable cells.

Ca^{2+}release from the intracellular Ca^{2+} stores may also favour formation of HCMD; the spatial coordinates of the Ca^{2+} channels of the stores are also restricted, as they can only locate at the ER membrane. In this case a specific HCMD topography can be favoured by the geometric disposition of the ER and its spatial relation to other organelles or morphological differentiations, for example mitochondria, nucleus or secretory vesicles (SV) [18, 50]. Finally local gradients of channel agonists, such as InsP3, must also synchronize the opening of Ca^{2+} channels that are physically close in space. Ca^{2+}-induced Ca^{2+} release (CICR), which is observed for both ryanodine receptors and InsP3 receptors [15], also tends to restrict the time span, thus increasing the probability of a HCMD.

Calcium entry by activation of VOCC. Coupling to transport by the endoplasmic reticulum

Ca^{2+} entry through VOCCs in chromaffin cells has been studied with great detail [29, 60, 63]. Membrane depolarisation to 0 mV elicits Ca^{2+} currents peaking near 800 pA that deactivate with a half-time of 300–500 ms. In bovine chromaffin cells, a depolarising stimulus lasting for 0.5 s typically elicits a mean I_{Ca} of 250 pA, which, in terms of Ca^{2+} flow, is equivalent to 700 μmol · l cells^{-1} · s^{-1} [63]. Measurements of ^{45}Ca uptake by bovine chromaffin cells depolarised with high K^+ during 5 s gave rates of $0.7 \cdot 10^{-15}$ μmol · l cells^{-1} · s^{-1}, which are equivalent to 400 μmol · l cells^{-1} · s^{-1} [9], a value reasonably consistent with the measured currents.

When we measured the rate of $[Ca^{2+}]_C$ increase in chromaffin cells depolarised with high K^+, we found values of 1 μmol · l cells^{-1} · s^{-1} [55]. This is only 1 of 700 of the estimated Ca^{2+} entry. Taking into account the binding to cytosolic Ca^{2+} buffers, we would expect a rate of 700/40= 17.5 μmol · l cells^{-1} · s^{-1}, which is still much larger than the measured value, suggesting that more than 90% of the entering Ca^{2+} is muffled [54] by transport out of the cytosol. Using aequorins targeted to different organelles delivered by a herpes virus [2], we were able to measure the contribution of the different transport processes [55]. Results are summarized in Fig. 1. The rate of Ca^{2+} entry was 700 μmol · l cells^{-1} · s^{-1}, but the $\Delta[Ca^{2+}]_C$ (taking into account cytosolic buffering) was only 40 μmol · l cells^{-1} · s^{-1}. The difference was due to pumping out Ca^{2+}: (1) to the extracellular medium through the plasma membrane (20–100 μmol · l cells^{-1} · s^{-1}); (2) inside ER (70–80 μmol · l cells^{-1} · s^{-1}); and (3) inside mitochondria, which is, by far, the largest component, more than 90% of the total entry (Fig. 1) [55].

Ca^{2+} transport by the ER is tricky because of the balance among uptake via the sarcoendoplasmic reticulum Ca^{2+} ATPase (SERCA) and release via CICR. Uptake by SERCA increases exponentially with $[Ca^{2+}]_C$ and can reach maximal rates 70–80 μmol · l cells^{-1} · s^{-1}, at 1–5 μM $[Ca^{2+}]_C$ [3, 55, 60]. At the steady state, the ER fills to a level of 500–1,000 μM $[Ca^{2+}]$. In this condition the rate of ER–cytosol Ca^{2+} exchange is about 2–3 μmol · l cells^{-1} · s^{-1}. Maximal stimulation of CICR with caffeine increases this leak 10–20 times [3, 55] and virtually empties of Ca^{2+} the ER. The stimulus for CICR is the sudden increase of $[Ca^{2+}]_C$. The threshold at which uptake via SERCA is substituted by release via CICR depends on several factors, including ER filling degree. Ca^{2+} entry via HVA Ca^{2+} channels activated by high K^+ depolarization is able to induce net Ca^{2+} release from the ER [3], suggesting that an HCMD high enough to activate CICR is formed near the sites of Ca^{2+} entry. This probably coexists in time with other more remote locations of the ER where the increase of $[Ca^{2+}]_C$ is insufficient to trigger Ca^{2+} release. Instead, net ER Ca^{2+} uptake resulting

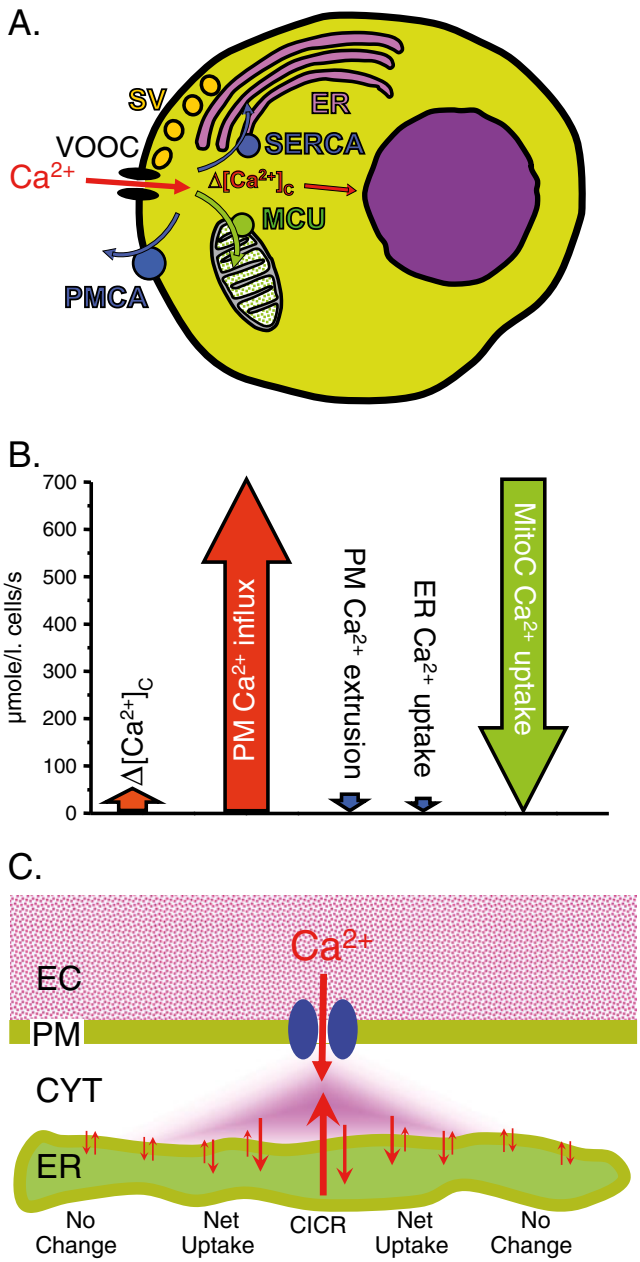

Fig. 1 Redistribution of Ca^{2+} entering through voltage-operated Ca^{2+} channels (*VOCC*) in chromaffin cells. **a** Ca^{2+} enters through VOCC and then it can be pumped back to the extracellular medium through plasma membrane Ca^{2+}-dependent ATPase (*PMCA*), taken up into the endoplasmic reticulum (*ER*) through the sarcoendoplasmic reticulum Ca^{2+}-dependent ATPase (*SERCA*) or into mitochondria via the mitochondrial calcium uniporter (*MCU*). *SV* secretory vesicles. **b** Compares transport through each transport system. *PM* plasma membrane. $\Delta[Ca^{2+}]_C$, increase of the cytosolic Ca^{2+} concentration, measured with fura-2. **c** Ca^{2+}-induced Ca^{2+} release (*CICR*). Ca^{2+} entering from the extracellular (*EC*) medium through VOCC of the plasma membrane (*PM*) generates a local hotspot that activates Ca^{2+} release from ER via the ryanodine receptor channel (*red arrow*), which amplifies the original signal. In other parts of the ER, there is net Ca^{2+} uptake via SERCA. *CYT* cytosol

from the increase of $[Ca^{2+}]_C$ would be observed at these locations (Fig. 1c). That is why CICR is so difficult to evidence and also why it is so efficient, as Ca^{2+} is released just over the target. In addition, Ca^{2+} missing the target is taken up again by ER and rereleased at the right place. Coupling of CICR to function is probably due to physical relationships.

Mitochondrial calcium transport

Chromaffin cell mitochondria accumulate large amounts of Ca^{2+} during stimulation with either high K^+ solutions, acetylcholine or caffeine [36]. Ca^{2+} is taken up through the mitochondrial Ca^{2+} uniporter (MCU), a protein associated to the inner mitochondrial membrane that has been cloned recently [12, 19] (Fig. 2a). MCU is a low-affinity/high-capacity system that uses the mitochondrial membrane potential (ψ_m) as the driving force for Ca^{2+} uptake [27]. Since ψ_m at rest is −150 to −180 mV, this transport system would promote accumulation of Ca^{2+} into the mitochondrial matrix up to five to six orders of magnitude above $[Ca^{2+}]_C$ at the thermodynamic equilibrium [13]. Ca^{2+} exit from mitochondria takes place through a Na^+/Ca^{2+} exchanger and also through a Na^+-independent system, the former being dominant in the adrenal medulla [27] (Fig. 2a). The *calcium-binding capacity* for Ca^{2+} (κ_S) inside the mitochondrial matrix seems to be very high, in the 10^3 range [11, 17, 29, 30]. In addition, it has been proposed recently that precipitation of $Ca_3(PO_4)_2$ into the matrix con account for additional, almost unlimited, buffering [16, 57].

It has been repeatedly reported that mitochondria can clear cytosolic Ca^{2+} loads in rat [11, 29, 57] and bovine chromaffin cells [36, 55, 60]. We have studied the kinetics of uptake by mitochondria in permeabilized bovine chromaffin cells infected with mitochondria-targeted aequorin probes [36, 55]. Measured mitochondrial uptake nicely fitted to the equation

$$v = \left\{ V_{max} \cdot \left([Ca^{2+}]_C \right)^2 \right\} / \left\{ (K_{50})^2 + \left([Ca^{2+}]_C \right)^2 \right\}$$

where V_{max}=158 µM · s^{-1} and K_{50}=23 µM. The K_{50} value is similar to both, the one obtained previously with isolated mitochondria from liver and heart and bovine adrenal medulla (10–15 µM) [26, 27] and the one estimated by Xu et al. [60] from measurements of the decrease of $[Ca^{2+}]_C$ in intact bovine chromaffin cells (40 µM). The value of V_{max} we estimate above would be equivalent to 6,320 µmol · l $cells^{-1}$ · s^{-1}, not far from the 4,800 value estimated by Xu et al. using an entirely different procedure based on clearance of Ca^{2+} photoreleased to the cytosol from a caged compound [60].

Because of the enormous driving force pushing Ca^{2+} from the cytosol towards the mitochondrial matrix, transport through the MCU is usually unidirectional. However, when the mitochondria depolarize, the electrochemical gradient

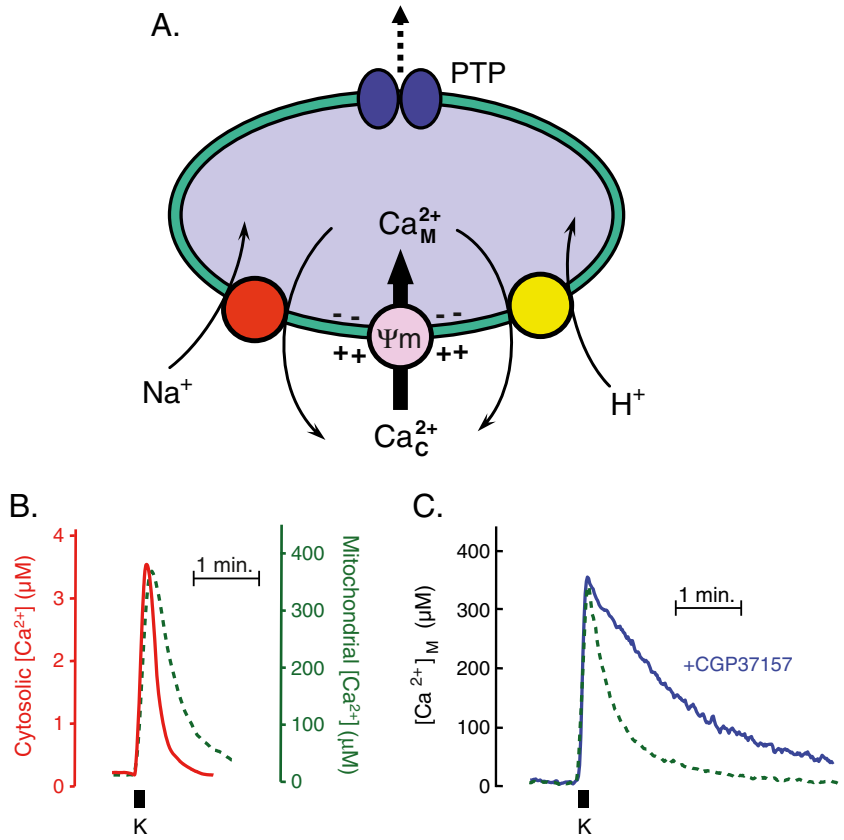

Fig. 2 Mitochondrial Ca^{2+} transport in chromaffin cells. **a** Scheme of the different mechanisms. Ca^{2+} entry happens via the mitochondrial uniporter, driven by the membrane potential (ψ_m). Exit happens via Na^+/Ca^{2+} exchange (*left*) and H^+/Ca^{2+} exchange (*right*). The permeability transition pore (*PTP*), which is normally closed, is shown on *top*. **b** Comparison of appearance of Ca^{2+} into the cytosol (*red trace*; scale at left; measured with fura-4F) and into the mitochondria (*green dotted trace*, scale at left, measured with low-affinity mitochondrial aequorin). Ca^{2+} entry was triggered by depolarization with high K^+ (70 mM; 10 s). **c** The Na^+/H^+ exchange inhibitor CGP37157 (20 μM; *blue trace*) blocks exit of Ca^{2+} from mitochondria in chromaffin cells

for Ca^{2+} collapses and the uniporter may mediate Ca^{2+} exit from the matrix of Ca^{2+}-loaded mitochondria. Under these circumstances, the increase of $[Ca^{2+}]_C$ may trigger the process and induce massive Ca^{2+} release, the so-called mitochondrial CICR (mCICR) [35]. Opening of the permeability transition pore (Fig. 2a) can also produce mCICR [31].

Under normal conditions, the exit of Ca^{2+} from Ca^{2+}-loaded mitochondria takes place mainly through the Na^+/Ca^{2+} exchanger (Fig. 2a) [26]. In our study with bovine chromaffin cells [55], mitochondrial release (at 37°C) had a sigmoidal kinetics that could be fitted by the following equation:

$$v = \left\{V_{max}\cdot\left(\left[Ca^{2+}\right]_M\right)^2\right\}/\left\{K_{50} + \left(\left[Ca^{2+}\right]_M\right)^2\right\}$$

with K_{50}=217 μM and V_{max}=20 μM/s, which would be equivalent to 780 $\mu mol \cdot l\,cells^{-1} \cdot s^{-1}$, one order of magnitude smaller than V_{max} for mitochondrial Ca^{2+} uptake (see above). Sigmoidicity disappeared at 22°C. The Na^+/Ca^{2+} exchanger inhibitor CGP37157 antagonized mitochondrial Ca^{2+} exit, both at 37°C and at 22°C [55].

Mitochondrial Ca^{2+} uptake during activation of adrenal chromaffin cells

Activation of chromaffin cells is started by activation of plasma membrane VOCC and Ca^{2+} entry. The resulting $[Ca^{2+}]_C$ peak is followed by a mitochondrial $[Ca^{2+}]_M$ increase (Fig. 2b). When stimulus ceases $[Ca^{2+}]_C$ relaxes and so does, with some delay, $[Ca^{2+}]_M$. Inhibitors of the Na^+/Ca^{2+} exchanger slows down mitochondrial Ca^{2+} clearance (Fig. 2c). The $[Ca^{2+}]_M$ peaks are then longer than the $[Ca^{2+}]_C$ counterparts. Since several NADH dehydrogenases are stimulated by Ca^{2+} in the micromolars range [27], the increase of $[Ca^{2+}]_M$ stimulates respiration and ATP synthesis [55] and this contributes to provide the energy needed to restore the perturbations generated during activation. The fact that the $[Ca^{2+}]_M$ peak is longer than the $[Ca^{2+}]_C$ one is a kind of "respiration debt" that secures restoration of the initial state. $[Ca^{2+}]_M$ can remain above micromolars levels for several minutes after cell stimulation [57].

The amount of calcium taken up into mitochondrial could be very large. During maximal stimulation of Ca^{2+} entry trough VOCC $[Ca^{2+}]_M$ peaks as high as 300–400 μM can be reached [36, 55] (Fig. 2b, c). Should all this Ca^{2+} be bound, this would make a $[^TCa]$ of 300–400 mM. A part of this calcium could precipitate as calcium phosphate into the mitochondrial matrix thus not generating osmotic stress [16, 57]. The value of the solubility product is compatible with the figures obtained here.

Note that the Ca^{2+} overload that enters through the plasma membrane during chromaffin cell stimulation is taken up preferentially by mitochondria, with very little uptake into ER (Fig. 1). This is to be expected from the characteristics

of Ca^{2+} transport by the different organelles in chromaffin cells. Figure 3 compares fluxes through VOCC (dotted line) with uptake by SERCA and mitochondria at different $[Ca^{2+}]_C$. At rest $[Ca^{2+}]_C$ of about 10^{-7} M (R in Fig. 3), there is no measurable uptake by mitochondria whereas SERCA works at 10–20% of V_{max}. Consequently Ca^{2+} accumulates into the ER at about 0.5–1 · 10^{-3} M. During maximal activation of VOOC, HDCA of 10^{-5} to 10^{-4} M $[Ca^{2+}]_C$ are formed near the plasma membrane Ca^{2+} channels [10, 38, 55]. Under these conditions (A2 in Fig. 3), Ca^{2+} is taken up mainly by mitochondria. Note that: (1) even though ER is accumulating Ca^{2+} at its V_{max}, the uptake by mitochondria is about 100-fold faster because of the high capacity of the mitochondrial uniporter; and (2) V_{max} of the uniporter is still ten times as large as the influx through VOCC and hence enough to muffle the Ca^{2+} overload (Fig. 3). We have demonstrated recently that, contrarily to what happens in chromaffin cells, the Ca^{2+} overload induced by activation of store-operated calcium entry (SOC; a plasma membrane channel that activates when the intracellular calcium stores are emptied) is taken up mainly into the ER in several cell models [6, 33, 34]. We attribute this difference to the fact that HCMD seen by mitochondria during activation of the SOC are smaller, in the 10^{-6} range (A1 in Fig. 3). This is enough to promote near maximal uptake into the ER, but uptake through the uniporter is relatively small (10–100 times slower).

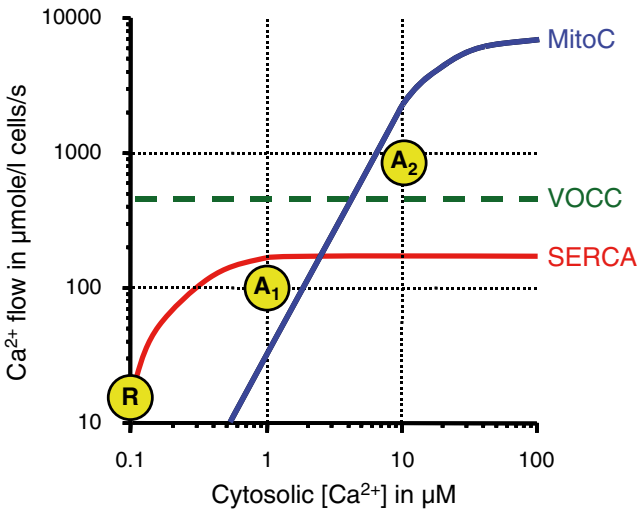

Fig. 3 Comparison of the concentration-dependence of several Ca^{2+} transport sytems. Entry through VOCC is fixed at 700 µmole· l cells^{-1} · s^{-1} (*green dotted* trace). Pumping through SERCA (*red trace*) and the uniporter (*blue trace*, labelled MitoC) were calculated using the equation: $v=\{V_{max} \cdot ([Ca^{2+}]_C)^2\}/\{(K_{50})^2+([Ca^{2+}]_C)^2\}$, with the following values for SERCA and the mitochondrial uniporter, respectively: V_{max}, 200 and 7,000 µmol · l cells^{-1} · s^{-1}, and K_{50}, 0.25 and 15 µM. Note double logarithmic scale. The *yellow circles* represent $[Ca^{2+}]_C$ levels attained at rest (*R*) and during activation, either close to VOCCs (A_2) or far away from them (A_1). Reproduced with permission from Villalobos et al. [55]

Two different mitochondrial Ca^{2+} pools are generated during activation of chromaffin cells

Measurements with aequorins allow to trace a memory of the Ca^{2+} changes, as the photoprotein is burned out in the compartments where $[Ca^{2+}]$ has been high. Our results suggest the existence of two different mitochondrial pools, M1 and M2, which take up Ca^{2+} at very different rates in response to activation of VOOCs. Pool M1 takes up Ca^{2+} at a rate of about 50 µM/s, 30% of uniporter's V_{max}, whereas uptake by pool M2 is about 150 times slower [36, 55]. According to the saturation kinetics parameters measured in chromaffin cells mitochondria, this corresponds to the rates obtained at about 20 and 2 µM $[Ca^{2+}]_C$, respectively. We believe that M1 corresponds to mitochondria close to the plasma membrane, which sense HCMD formed close to the mouth of VOCC and takes up very large amounts of calcium, thus muffling the progression of the Ca^{2+} wave towards the cell core (Fig. 4a). Since the sphere volume increases more than surface on moving away from the centre, the pool M1, containing 50% of mitochondria, would occupy a deepness of less than 2 µm below the plasma membrane in a 15-µm diameter cell (corresponding to the dotted subplasmalemmal area in Fig. 4a). This mitochondrial pool would accumulate most of the entering Ca^{2+} load whereas pool M2, at the cell core, would sense much smaller $[Ca^{2+}]_C$ and take up a minor fraction of the load. Electron microscopy X-ray microanalysis of frog sympathetic neurons after stimulation with high K^+ also revealed the existence of two mitochondrial pools with different Ca^{2+} contents [46] and so did aequorin in mouse sympathetic neurons [41] and pancreatic beta cells [48]. In pancreatic acinar cells, entry of Ca^{2+} through plasma membrane also caused preferential Ca^{2+} uptake into subplasmalemmal mitochondria [42].

Functional triads composed by VOCC, CICR and subplasmalemmal mitochondria generate HCMD that optimize coupling to secretion

As pointed out above, the $[Ca^{2+}]_C$ signals generated by activation of VOCC can be amplified by CICR in chromaffin cells [3]. Strategic location of VOCC, CICR sites and the mitochondrial M1 pool conforming functional triads is essential for maximizing HCMD and optimizing secretion [24, 36] (Fig. 4b). Thus $[Ca^{2+}]_C$ hotspots reach concentrations of as high as 50 µM at the subplasmalemmal region, where SV are docked. VOCC is the trigger, CICR the amplifier and then subplasmalemmal mitochondria (M1) act as a contention wall that accumulates calcium and avoids propagation of the calcium wave towards the cell core. The increase of $[Ca^{2+}]_M$ stimulates respiration [26, 27, 32, 47], thus tuning local energy production to the increased needs of the

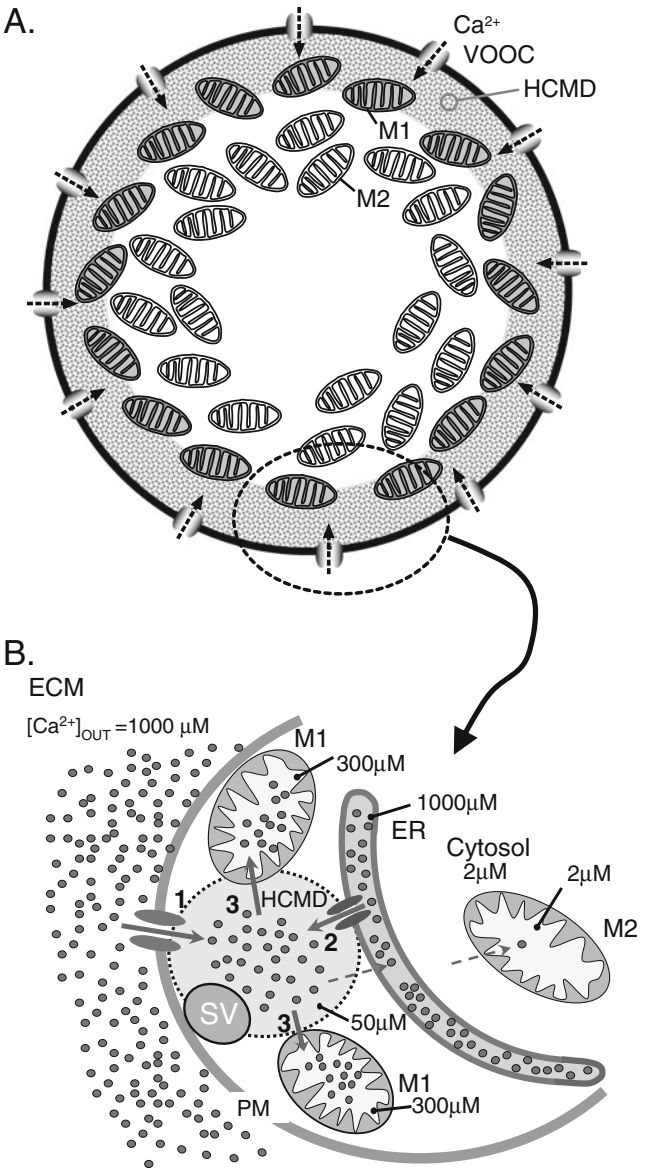

Fig. 4 Spatial disposition of mitochondria in chromaffin cells. **a** Ca^{2+} enters through activated VOCC (*arrows*) and generates a high Ca^{2+} microdomain in the subplasmalemmal region (*dotted area*). Mitochondria close to plasma membrane (*M1*) take up large amounts of Ca^{2+} and stop progression of the $[Ca^{2+}]_C$ wave towards the cell core. Deeper mitochondria (*M2*) take up much less calcium, as $[Ca^{2+}]_C$ in their vicinity is well below K_{50} of the mitochondrial Ca^{2+} uniporter. Aequorin is burned much faster in M1 than in M2 mitochondria. **b** Detail showing functional triads that modulate local high $[Ca^{2+}]_C$ microdomains. Ca^{2+} enters through VOCC (*1*) and generates a high $[Ca^{2+}]_C$ domain, which is amplified by Ca^{2+} release from the ER (*2*). The surrounding mitochondria (*M1*) avoid lateral progress of the Ca^{2+} wave by taking up Ca^{2+} (*3*). Note that ER does also avoid progression of the wave towards the cell core. Deeper mitochondria see much smaller concentrations of Ca^{2+} and do not accumulate it in their matrix (*M2*). The approximate Ca^{2+} concentrations in the extracellular medium (*ECM*), high Ca^{2+} microdomain (*HCMD*), mitochondrial matrix of pools M1 and M2 and ER lumen and bulk cytosol are shown in the figure. *PM* plasma membrane. Note that docked secretory vesicles (*SV*) are easily reached by the HCMD

exocytic activity. Respiratory stimulation will lag behind cessation of activity until the mitochondrial calcium load is completely cleared, and this may take several minutes [57]. Much of the Ca^{2+} that enters mitochondria at subplasmalemmal locations may diffuse through the mitochondrial matrix to other cell locations and, eventually, be extruded from mitochondria near the cell core. This mitochondrial Ca^{2+} release probably contributes to keep $[Ca^{2+}]_C$ discretely raised during the poststimulus period, perhaps facilitating the transport of new vesicles to refill the readily releasable pool [56].

If the location or the Ca^{2+} handling properties of mitochondria in these functional triads could be regulated, this could be an effective mechanism for modulation of the exocytotic process. If these mechanisms could be extrapolated to neurons, these changes of these functional triads could contribute to modulation of synaptic plasticity. Finally, under brain stress conditions, such as excitotoxicity or ischemia–reperfusion damage, ageing or development of neurodegenerative diseases, mitochondrial dysfunction may reduce the ability of the mitochondria to muffle cytosolic Ca^{2+}, this leading to increased secretion of excitatory neurotransmitters and cell overactivation, a vicious circle that may trigger processes leading to cell death [14]. Changes in CICR could also modulate the synaptic efficacy under physiological or pathophysiological conditions.

Concluding remarks

Since Douglas and Rubin [21] showed, in1961, that Ca^{2+} entry was the only requirement to trigger the acetylcholine-mediated release of catecholamines from the adrenal gland, we have learned much about basic and molecular aspects of Ca^{2+} signalling and exocytosis in chromaffin cells. The physiologically relevant intracellular Ca^{2+} signals occur either as localized hot spots of high Ca^{2+} concentration or as propagating Ca^{2+} waves, which give rise to global Ca^{2+} elevations. The cytoplasmic organelles are essential for shaping the $[Ca^{2+}]_C$ signals in order to optimize stimulus secretion coupling. Our results suggest a highly structured spatiotemporal organization of the Ca^{2+} signals originated by sustained Ca^{2+} entry through VOCC. High $[Ca^{2+}]_C$ microdomains suitable for triggering exocytosis are generated only at the subplasmalemmal region. Domains with a much smaller $[Ca^{2+}]_C$ increase but more sustained in time, perhaps adequate for mobilizing the reserve pool of secretory vesicles, are generated at the core regions of the cytosol and at the nucleus. Mitochondria are essential for shaping adequately these local Ca^{2+} domains. And, on the other hand, Ca^{2+} uptake by mitochondria activates NADH dehydrogenases, thus tuning up respiration to match the increased local energy needs. Full relaxation of the $[Ca^{2+}]_C$

peak requires clearance of the mitochondrial Ca^{2+} load through the Na^{+}/Ca^{2+} exchanger, which proceeds slowly at low micromolar $[Ca^{2+}]_M$ levels. This keeps respiration stimulated and core $[Ca^{2+}]_C$ discretely high for a long period after stimulation, acting as a kind of memory that may help to secure restoration of the initial conditions. Mitochondrial dysfunction impairs calcium homeostasis and stimulus–secretion coupling, and may contribute to generation of excitotoxic or neurodegenerative disorders.

Acknowledgements Financial support from the following institutions is gratefully acknowledged: To JGS, grants from the EU-ERA-Net program and the Spanish Ministerio de Ciencia e Innovación (MICINN), SAF2008-03175-E and BFU2010-17379, Red de Terapia Celular, Instituto de Salud Carlos III (RD06/0010/0000) and the Junta de Castilla y León (gr175). To AGG, SAF2010-21795 (MCINN); RETICS RD06/0009, Instituto de Salud Carlos III; (3) S-SAL-0275-2006, Comunidad Autónoma de Madrid; NDG07/9 y NDG09/8, Agencia Laín Entralgo, Comunidad Autónoma de Madrid, Spain; Fundación Teófilo Hernando.

References

1. Albrecht MA, Colegrove SL, Friel DD (2002) Differential regulation of ER Ca^{2+} uptake and release rates accounts for multiple modes of Ca^{2+}-induced Ca^{2+} release. J Gen Physiol 119:211–233
2. Alonso MT, Barrero MJ, Carnicero E, Montero M, Garcia-Sancho J, Alvarez J (1998) Functional measurements of $[Ca^{2+}]$ in the endoplasmic reticulum using a herpes virus to deliver targeted aequorin. Cell Calcium 24:87–96
3. Alonso MT, Barrero MJ, Michelena P, Carnicero E, Cuchillo I, Garcia AG, Garcia-Sancho J, Montero M, Alvarez J (1999) Ca^{2+}-induced Ca^{2+} release in chromaffin cells seen from inside the ER with targeted aequorin. J Cell Biol 144:241–254
4. Alonso MT, Garcia-Sancho J (2011) Nuclear Ca(2+) signalling. Cell Calcium 49:280–289
5. Alonso MT, Manjarres IM, Garcia-Sancho J (2009) Modulation of calcium signalling by intracellular organelles seen with targeted aequorins. Acta Physiol (Oxf) 195:37–49
6. Alonso MT, Manjarres IM, Garcia-Sancho J (2012) Privileged coupling between Ca(2+) entry through plasma membrane store-operated Ca(2+) channels and the endoplasmic reticulum Ca(2+) pump. Mol Cell Endocrinol (in press)
7. Alonso MT, Villalobos C, Chamero P, Alvarez J, Garcia-Sancho J (2006) Calcium microdomains in mitochondria and nucleus. Cell Calcium 40:513–525
8. Alvarez J, Montero M, Garcia-Sancho J (1999) Subcellular Ca(2+) dynamics. News Physiol Sci 14:161–168
9. Artalejo CR, Garcia AG, Aunis D (1987) Chromaffin cell calcium channel kinetics measured isotopically through fast calcium, strontium, and barium fluxes. J Biol Chem 262:915–926
10. Augustine GJ, Neher E (1992) Calcium requirements for secretion in bovine chromaffin cells. J Physiol 450:247–271
11. Babcock DF, Herrington J, Goodwin PC, Park YB, Hille B (1997) Mitochondrial participation in the intracellular Ca^{2+} network. J Cell Biol 136:833–844
12. Baughman JM, Perocchi F, Girgis HS, Plovanich M, Belcher-Timme CA, Sancak Y, Bao XR, Strittmatter L, Goldberger O, Bogorad RL, Koteliansky V, Mootha VK (2011) Integrative genomics identifies MCU as an essential component of the mitochondrial calcium uniporter. Nature 476:341–345
13. Bernardi P (1999) Mitochondrial transport of cations: channels, exchangers, and permeability transition. Physiol Rev 79:1127–1155
14. Berridge MJ (2011) Calcium signalling and Alzheimer's disease. Neurochem Res 36:1149–1156
15. Berridge MJ, Lipp P, Bootman MD (2000) The versatility and universality of calcium signalling. Nat Rev Mol Cell Biol 1:11–21
16. Chalmers S, Nicholls DG (2003) The relationship between free and total calcium concentrations in the matrix of liver and brain mitochondria. J Biol Chem 278:19062–19070
17. Coll KE, Joseph SK, Corkey BE, Williamson JR (1982) Determination of the matrix free Ca^{2+} concentration and kinetics of Ca^{2+} efflux in liver and heart mitochondria. J Biol Chem 257:8696–8704
18. Csordas G, Hajnoczky G (2003) Plasticity of mitochondrial calcium signaling. J Biol Chem 278:42273–42282
19. De Stefani D, Raffaello A, Teardo E, Szabo I, Rizzuto R (2011) A forty-kilodalton protein of the inner membrane is the mitochondrial calcium uniporter. Nature 476:336–340
20. Douglas WW (1968) Stimulus-secretion coupling: the concept and clues from chromaffin and other cells. Br J Pharmacol 34:451–474
21. Douglas WW, Rubin RP (1961) The role of calcium in the secretory response of the adrenal medulla to acetylcholine. J Physiol 159:40–57
22. Duchen MR, Szabadkai G (2010) Roles of mitochondria in human disease. Essays Biochem 47:115–137
23. Friel DD, Tsien RW (1994) An FCCP-sensitive Ca^{2+} store in bullfrog sympathetic neurons and its participation in stimulus-evoked changes in $[Ca^{2+}]$i. J Neurosci 14:4007–4024
24. Garcia AG, Garcia-De-Diego AM, Gandia L, Borges R, Garcia-Sancho J (2006) Calcium signaling and exocytosis in adrenal chromaffin cells. Physiol Rev 86:1093–1131
25. Garcia-Sancho J, Verkhratsky A (2008) Cytoplasmic organelles determine complexity and specificity of calcium signalling in adrenal chromaffin cells. Acta Physiol (Oxf) 192:263–271
26. Gunter TE, Gunter KK, Sheu SS, Gavin CE (1994) Mitochondrial calcium transport: physiological and pathological relevance. Am J Physiol 267:C313–C339
27. Gunter TE, Pfeiffer DR (1990) Mechanisms by which mitochondria transport calcium. Am J Physiol 258:C755–C786
28. Haigh JR, Parris R, Phillips JH (1989) Free concentrations of sodium, potassium and calcium in chromaffin granules. Biochem J 259:485–491
29. Herrington J, Park YB, Babcock DF, Hille B (1996) Dominant role of mitochondria in clearance of large Ca^{2+} loads from rat adrenal chromaffin cells. Neuron 16:219–228
30. Horikawa Y, Goel A, Somlyo AP, Somlyo AV (1998) Mitochondrial calcium in relaxed and tetanized myocardium. Biophys J 74:1579–1590
31. Ichas F, Jouaville LS, Mazat JP (1997) Mitochondria are excitable organelles capable of generating and conveying electrical and calcium signals. Cell 89:1145–1153
32. Maechler P, Wollheim CB (1998) Role of mitochondria in metabolism-secretion coupling of insulin release in the pancreatic beta-cell. Biofactors 8:255–262
33. Manjarres IM, Alonso MT, Garcia-Sancho J (2011) Calcium entry-calcium refilling (CECR) coupling between store-operated Ca(2+) entry and sarco/endoplasmic reticulum Ca(2+)-ATPase. Cell Calcium 49:153–161
34. Manjarres IM, Rodriguez-Garcia A, Alonso MT, Garcia-Sancho J (2010) The sarco/endoplasmic reticulum Ca(2+) ATPase (SERCA) is the third element in capacitative calcium entry. Cell Calcium 47:412–418
35. Montero M, Alonso MT, Albillos A, Garcia-Sancho J, Alvarez J (2001) Mitochondrial Ca(2+)-induced Ca(2+) release mediated by the Ca(2+) uniporter. Mol Biol Cell 12:63–71

36. Montero M, Alonso MT, Carnicero E, Cuchillo-Ibanez I, Albillos A, Garcia AG, Garcia-Sancho J, Alvarez J (2000) Chromaffin-cell stimulation triggers fast millimolar mitochondrial Ca^{2+} transients that modulate secretion. Nat Cell Biol 2:57–61
37. Naraghi M, Müller TH, Neher E (1998) Two-dimensional determination of the cellular Ca^{2+} binding in bovine chromaffin cells. Biophys J 75:1635–1647
38. Neher E (1998) Vesicle pools and Ca^{2+} microdomains: new tools for understanding their roles in neurotransmitter release. Neuron 20:389–399
39. Neher E (1998) Usefulness and limitations of linear approximations to the understanding of Ca++ signals [published erratum appears in Cell Calcium 1999 Mar;25(3):275]. Cell Calcium 24:345–357
40. Neher E, Augustine GJ (1992) Calcium gradients and buffers in bovine chromaffin cells. J Physiol 450:273–301
41. Nunez L, Senovilla L, Sanz-Blasco S, Chamero P, Alonso MT, Villalobos C, Garcia-Sancho J (2007) Bioluminescence imaging of mitochondrial Ca^{2+} dynamics in soma and neurites of individual adult mouse sympathetic neurons. J Physiol 580:385–395
42. Park MK, Ashby MC, Erdemli G, Petersen OH, Tepikin AV (2001) Perinuclear, perigranular and sub-plasmalemmal mitochondria have distinct functions in the regulation of cellular calcium transport. EMBO J 20:1863–1874
43. Patel S, Muallem S (2011) Acidic Ca(2+) stores come to the fore. Cell Calcium 50:109–112
44. Petersen OH, Tepikin AV (2008) Polarized calcium signaling in exocrine gland cells. Annu Rev Physiol 70:273–299
45. Phillips JH, Allison YP, Morris SJ (1977) The distribution of calcium, magnesium, copper and iron in the bovine adrenal medulla. Neuroscience 2:147–152
46. Pivovarova NB, Hongpaisan J, Andrews SB, Friel DD (1999) Depolarization-induced mitochondrial Ca accumulation in sympathetic neurons: spatial and temporal characteristics. J Neurosci 19:6372–6384
47. Pralong WF, Hunyady L, Varnai P, Wollheim CB, Spat A (1992) Pyridine nucleotide redox state parallels production of aldosterone in potassium-stimulated adrenal glomerulosa cells. Proc Natl Acad Sci U S A 89:132–136
48. Quesada I, Villalobos C, Nunez L, Chamero P, Alonso MT, Nadal A, Garcia-Sancho J (2008) Glucose induces synchronous mitochondrial calcium oscillations in intact pancreatic islets. Cell Calcium 43:39–47
49. Rizzuto R, Bernardi P, Pozzan T (2000) Mitochondria as all-round players of the calcium game. J Physiol 529(Pt 1):37–47
50. Rizzuto R, Pinton P, Carrington W, Fay FS, Fogarty KE, Lifshitz LM, Tuft RA, Pozzan T (1998) Close contacts with the endoplasmic reticulum as determinants of mitochondrial Ca^{2+} responses. Science 280:1763–1766
51. Rutter GA, Theler JM, Murgia M, Wollheim CB, Pozzan T, Rizzuto R (1993) Stimulated Ca^{2+} influx raises mitochondrial free Ca^{2+} to supramicromolar levels in a pancreatic beta-cell line. Possible role in glucose and agonist-induced insulin secretion. J Biol Chem 268:22385–22390
52. Sala F, Hernandez-Cruz A (1990) Calcium diffusion modeling in a spherical neuron. Relevance of buffering properties. Biophys J 57:313–324
53. Santodomingo J, Vay L, Camacho M, Hernandez-Sanmiguel E, Fonteriz RI, Lobaton CD, Montero M, Moreno A, Alvarez J (2008) Calcium dynamics in bovine adrenal medulla chromaffin cell secretory granules. Eur J Neurosci 28:1265–1274
54. Schwiening CJ, Thomas RC (1996) Relationship between intracellular calcium and its muffling measured by calcium iontophoresis in snail neurones. J Physiol 491(Pt 3):621–633
55. Villalobos C, Nunez L, Montero M, Garcia AG, Alonso MT, Chamero P, Alvarez J, Garcia-Sancho J (2002) Redistribution of Ca^{2+} among cytosol and organella during stimulation of bovine chromaffin cells. FASEB J 16:343–353
56. von Ruden L, Neher E (1993) A Ca-dependent early step in the release of catecholamines from adrenal chromaffin cells. Science 262:1061–1065
57. Warashina A (2006) Mode of mitochondrial Ca^{2+} clearance and its influence on secretory responses in stimulated chromaffin cells. Cell Calcium 39:35–46
58. Wendt-Gallitelli MF, Isenberg G (1991) Total and free myoplasmic calcium during a contraction cycle: X-ray microanalysis in guinea-pig ventricular myocytes. J Physiol 435:349–372
59. Winkler H, Westhead E (1980) The molecular organization of adrenal chromaffin granules. Neuroscience 5:1803–1823
60. Xu T, Naraghi M, Kang H, Neher E (1997) Kinetic studies of Ca^{2+} binding and Ca^{2+} clearance in the cytosol of adrenal chromaffin cells. Biophys J 73:532–545
61. Yoo SH (2010) Secretory granules in inositol 1,4,5-trisphosphate-dependent Ca^{2+} signaling in the cytoplasm of neuroendocrine cells. FASEB J 24:653–664
62. Yoo SH, Chu SY, Kim KD, Huh YH (2007) Presence of secretogranin II and high-capacity, low-affinity Ca^{2+} storage role in nucleoplasmic Ca^{2+} store vesicles. Biochemistry 46:14663–14671
63. Zhou Z, Neher E (1993) Mobile and immobile calcium buffers in bovine adrenal chromaffin cells. J Physiol 469:245–273